

Electronic Supplementary Information (ESI)

Synthesis of poly(styrene-*b*-4-(*tert*-butyldimethylsiloxy)styrene) block copolymers and characterization of their self-assembled patterns

Yoon Hyung Hur,^{‡a} Seungwon Song,^{‡a} Jimmy Mays,^b YongJoo Kim,^{*c} Beom-Goo Kang,^{*b} and Yeon Sik Jung^{*a}

^a Department of Materials Science and Engineering, Korea Advanced Institute of Science and Technology (KAIST), 291 Daehak-ro, Yuseong-gu, Daejeon 302-701, Republic of Korea

^b Department of Chemistry, University of Tennessee, Knoxville, Tennessee 37996, United States

^c KI for NanoCentury, Korea Advanced Institute of Science and Technology (KAIST), 291 Daehak-ro, Yuseong-gu, Daejeon 302-701, Republic of Korea

[‡] These authors equally contributed to this work.

Table S1. Synthesis results of PS-*b*-P4BDSS by anionic polymerization

sample	s-BuLi ^a mmol	block copolymer (homopolymer)					domain size ^e nm	morphology ^f		
		monomer		$M_n \times 10^{-3}$		M_w/M_n^d				
		1 st , mmol	2 nd , mmol	calcd ^b	obsd ^c					
A-13	0.090	A, 5.99	B, 1.78	11.7 (6.9)	12.5 (7.5)	1.01 (1.02)	-	DIS		
A-54	0.021	A, 7.48	B, 1.53	53.2 (36.5)	54.2 (37.1)	1.05 (1.06)	38.3	CYL		
A-33	0.032	A, 7.04	B, 1.41	32.3 (22.0)	33.2 (22.9)	1.03 (1.04)	21.5	CYL		
A-25	0.015	A, 6.20	B, 1.27	24.0 (17.1)	25.3 (16.3)	1.01 (1.05)	16.4	CYL		
A-117	0.020	A, 12.0	B, 2.41	93.8 (62.4)	116.6 (63.0)	1.06 (1.12)	54.8	LAM		
A-30	0.028	A, 3.84	B, 1.95	32.6 (14.3)	29.8 (15.9)	1.03 (1.01)	20.3	LAM		
A-27	0.041	A, 7.95	B, 1.21	25.4 (19.1)	26.8 (19.9)	1.01 (1.03)	18.9	CYL + HPL		

^a sec-Butyllithium used as initiator of anionic polymerization. ^b M_n (calcd) = (molecular weight of monomer) \times [monomer] / [initiator]. ^c M_n of the block copolymer was determined by using M_n of poly(A) and the molar ratio of each block estimated by ¹H NMR. ^d M_w/M_n was determined by using SEC calibration with PS standards in a THF solution containing 2% triethylamine as the eluent at 40 °C. ^e Domain size of BCPs was measured by bulk SAXS. ^f Morphology of BCPs was confirmed by bulk SAXS, where DIS: disorder, CYL: cylinder, LAM: lamellae, and HPL: Hexagonally perforated lamellae.

Table S2. Synthesis results of PS-*b*-P4BDSS by RAFT polymerization

sample	RAFT ^a	AIBN	block copolymer (homopolymer)			M_w/M_n^d	domain size ^e nm	morphology ^f
			monomer		$M_n \times 10^{-3}$			
			Mmol	Mmol	1 st , mmol	2 nd , mmol	obsd ^c	
R-55	0.021	0.011	A, 3.62	B, 2.30	55.1 (36.3)	1.14 (1.21)	-39.2	CYL
R-54	0.021	0.011	A, 3.62	B, 2.33	54.3 (36.3)	1.32 (1.21)	39.2	CYL
R-25	0.020	0.010	A, 1.64	B, 1.13	25.2 (16.2)	1.15 (1.17)	16.5	CYL
R-26	0.020	0.010	A, 1.64	B, .115	25.7 (16.2)	1.21 (1.17)	16.8	CYL

^a sec-Butyllithium used as initiator of anionic polymerization. ^b M_n of the block copolymer was determined by using M_n of poly(A) and the molar ratio of each block estimated by 1H NMR. ^c M_w/M_n was determined by using SEC calibration with PS standards in a THF solution containing 2% triethylamine as the eluent at 40 °C. ^d Domain size of BCPs was measured by bulk SAXS. ^e Morphology of BCPs was confirmed by bulk SAXS, where DIS: disorder, CYL: cylinder, LAM: lamellae, and HPL: Hexagonally perforated lamellae.

Table S3. Pattern quality comparison between various BCPs with different χ .

	CD (nm)	χ	PDI	LER (nm)	LWR (nm)	Annealing Methods
PS- <i>b</i> -PMMA ^a	10.5 ^d	0.0324	1.06	4.85 \pm 0.71	-	Thermal Annealing
PS- <i>b</i> -P4BDSS	11.4	0.0525	1.01	3.25 \pm 0.54	3.02 \pm 0.28	Thermal Annealing
	18.4		1.14	3.41 \pm 0.85	2.85 \pm 0.48	Thermal Annealing
PS- <i>b</i> -PDMS ^b	13.6	0.0950	1.09	4.83 \pm 0.19	4.11 \pm 0.23	Solvent Annealing
	13.3			2.85 \pm 0.12	2.54 \pm 0.16	Solvothermal Annealing
P4VP- <i>b</i> -PDMS ^c	17.6	0.6650	1.25	1.88 \pm 0.17	0.98 \pm 0.07	Solvothermal Annealing

^a According to K. S. Lee *et al*, *ACS Applied Materials & Interfaces*, 2017. **9**, 31245-31251. ^b According to J. M. Kim *et al*, *Advanced Functional Materials*, 2015, **25**, 306-315. ^c According to J. M. Kim *et al*, *Chemistry of Materials*, 2016, **28**, 5680-5688. ^d CD of PS-*b*-PMMA was calculated by half of domain size.

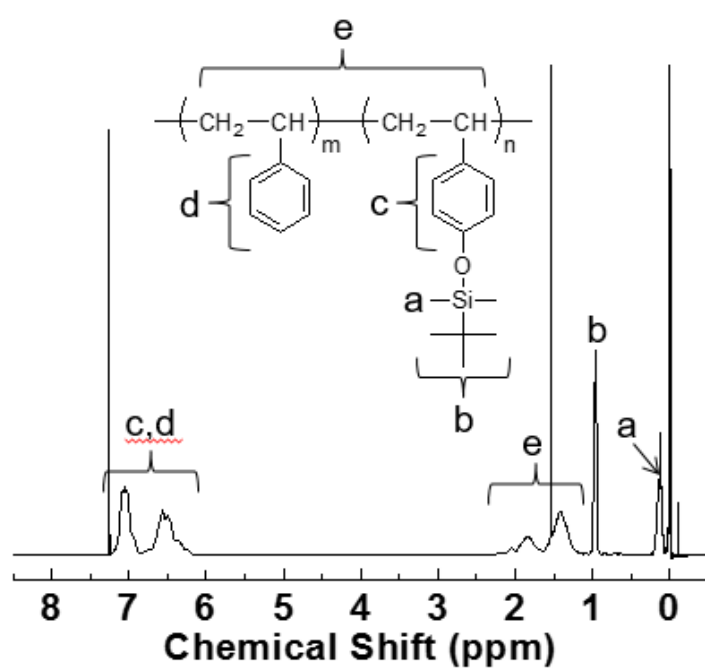


Figure S1. Characteristics of ^1H NMR of PS-*b*-P4BDSS

According to **Leibler's mean-field theory**,

$$I(q) = K[S(q) / W(q) - 2\chi]^{-1}$$

where K is a proportionality constant which is not important in the present work and is defined in the text.

$$S(q) = \langle S_{x,x}(q) \rangle_v + 2 \langle S_{x,y}(q) \rangle_v + \langle S_{y,y}(q) \rangle_v$$

$$W(q) = \langle S_{x,x}(q) \rangle_v * \langle S_{y,y}(q) \rangle_v - \langle S_{y,y}(q) \rangle_v^2$$

where,

$$\langle S_{x,x}(q) \rangle_v = r_{c,n} f_x^2 g_{x,n}^{(2)}(q)$$

$$\langle S_{x,y}(q) \rangle_v = r_{c,n} f_x f_y g_{x,n}^{(1)}(q) g_{y,n}^{(1)}(q)$$

$$r_{c,n} = (v_x N_{x,n} + v_y N_{y,n}) / (v_x * v_y)^{1/2}$$

$$g_{x,n}^{(1)}(q) = 1/x_{x,n} \{ 1 - [x_{x,n} (\lambda_x - 1) + 1]^{-\lambda_x} \}^{-1}$$

$$g_{x,n}^{(2)}(q) = 1/x_{x,n}^2 \{ -1 + [x_{x,n} (\lambda_x - 1) + 1]^{-\lambda_x} \}^{-1}$$

$$x_{x,n} = (N_{x,w} b_x^2 / 6) q^2$$

$$\lambda_{x,n} = N_{x,w} / N_{x,n}$$

v_x is molecular volume of X (cm³/mol). f_x is the volume fraction of X. $N_{x,n}$ and $N_{x,w}$ is the number-average and weight-average degree of polymerization of X block chain. b_x is the segment length of X.

Figure S2. Calculation of chi in PS-*b*-P4BDSS

	w (weight fraction)	f (volume fraction)	N (repeating unit)	b (segment length)	v (molar volume)	λ (PDI)
PS	0.600	0.634	72.0	0.57	98.6	1.03
P4BDSS	0.400	0.366	21.3	0.47	194	1.10

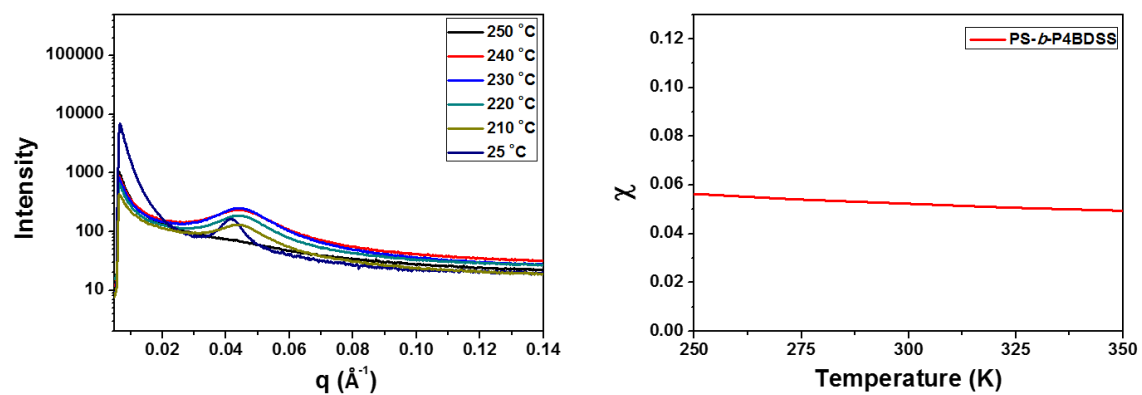


Figure S3. Calculation of χ in poly PS-*b*-P4BDSS

	w (weight fraction)	f (volume fraction)	N (repeating unit)	b (segment length)	v (molar volume)	λ (PDI)
PMMA	0.500	0.468	179.78	0.488	84.84	1.54
PS	0.500	0.532	172.83	0.681	100.14	1.18

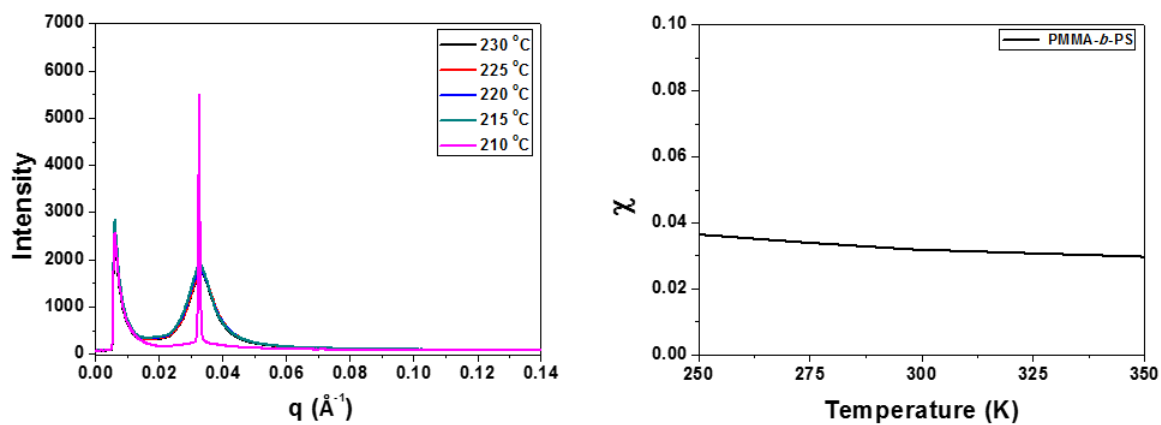


Figure S4. Calculation of χ in PS-*b*-PMMA (34k)

	w (weight fraction)	f (volume fraction)	N (repeating unit)	b (segment length)	v (molar volume)	λ (PDI)
PDMS	0.487	0.319	31.02	0.712	104.14	1.13
PS	0.513	0.681	50.12	0.681	138.50	1.76

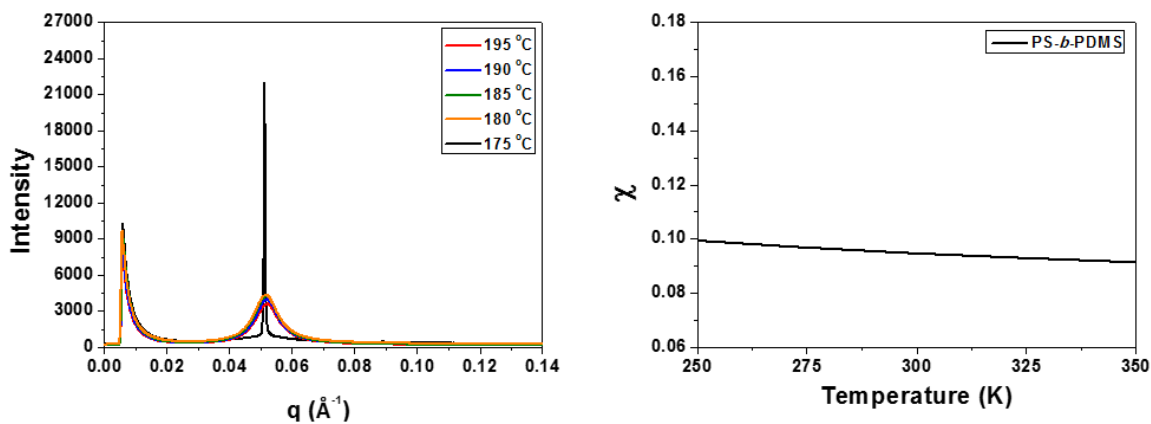


Figure S5. Calculation of χ in PS-*b*-PDMS

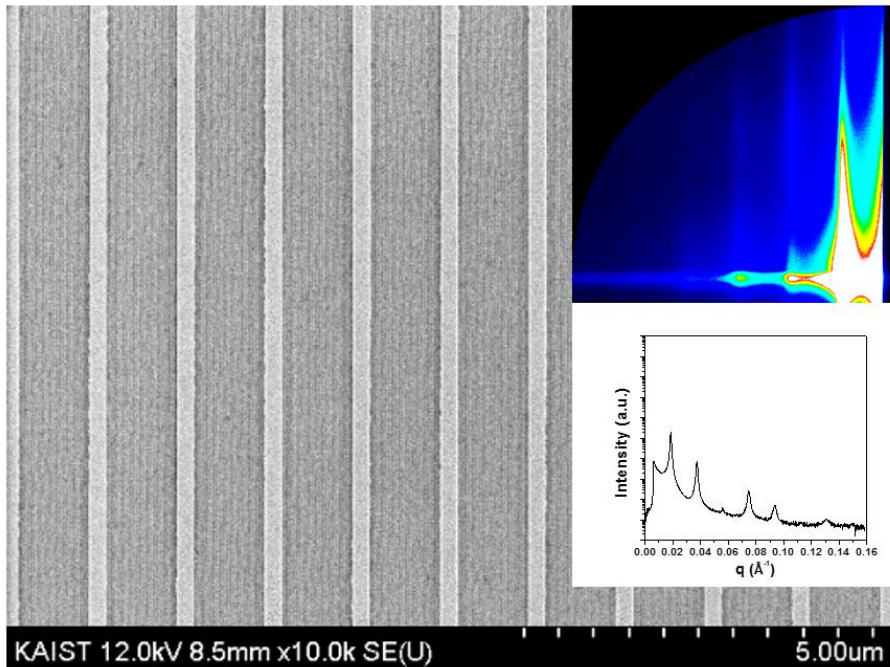


Figure S6. SEM and GISAXS measurements of A-54

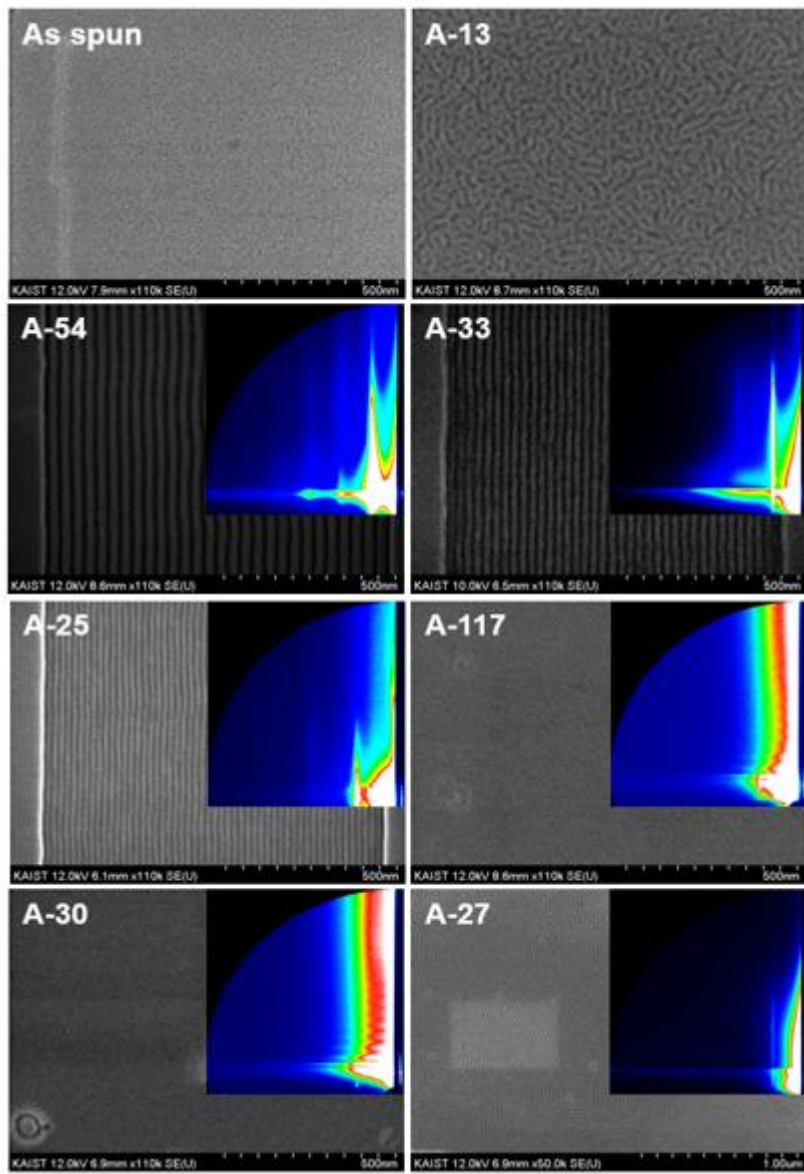


Figure S7. Self-assembly of PS-*b*-P4BDSS at 200 °C for 1h.

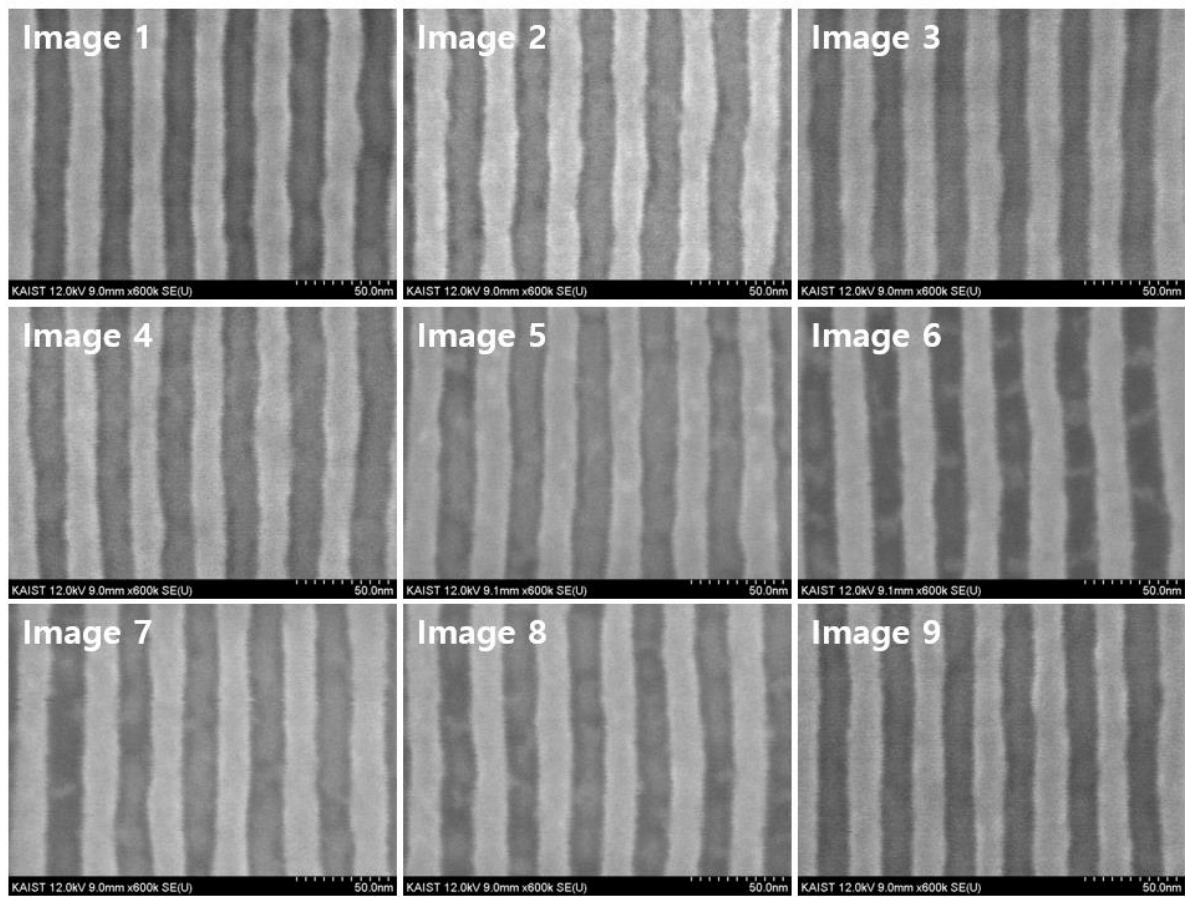


Figure S8. Pattern quality analysis of A-54

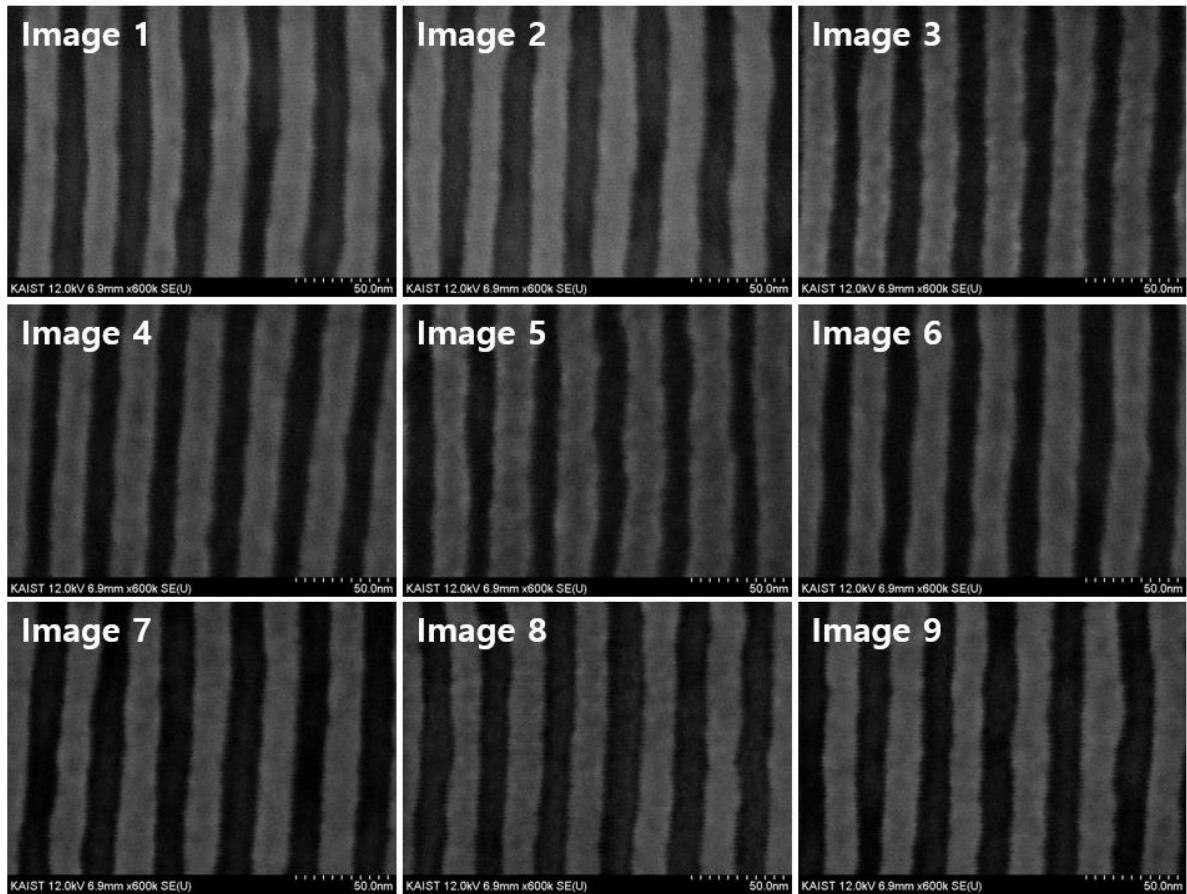


Figure S9. Pattern quality analysis of R-55

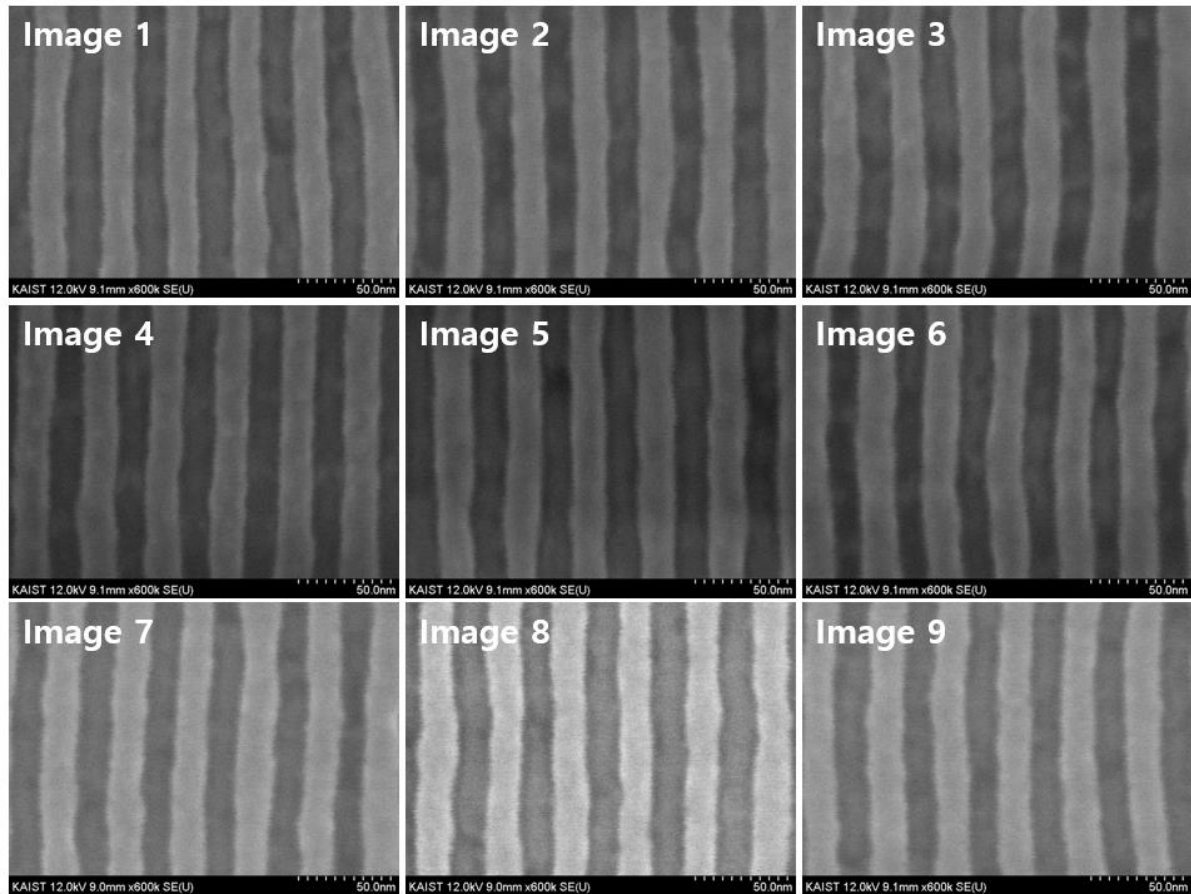
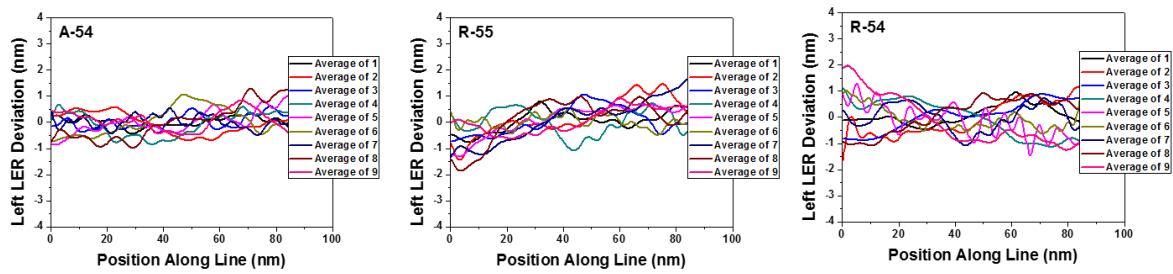


Figure S10. Pattern quality analysis of R-54

(a) Left LER analysis



(b) Right LER analysis

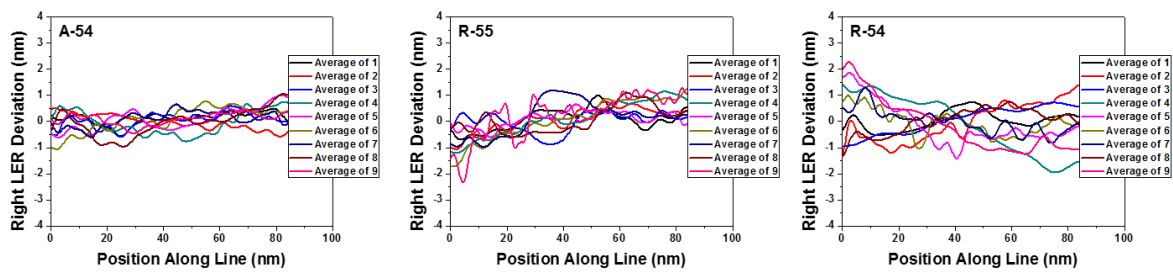


Figure S11. LER comparison of PS-*b*-P4BDSS

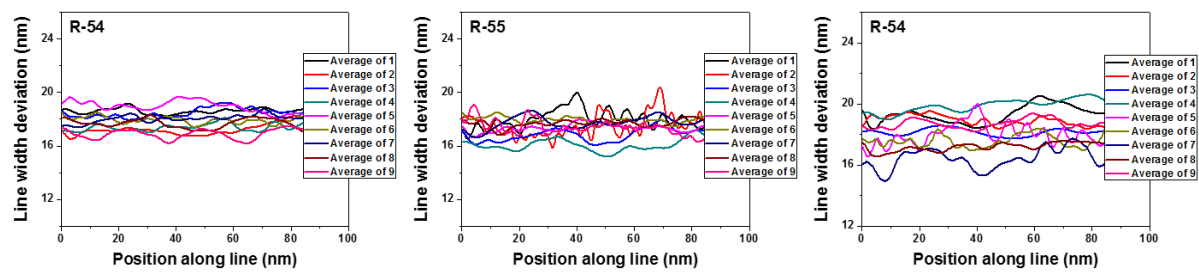


Figure S12. LWR comparison of PS-*b*-P4BDSS

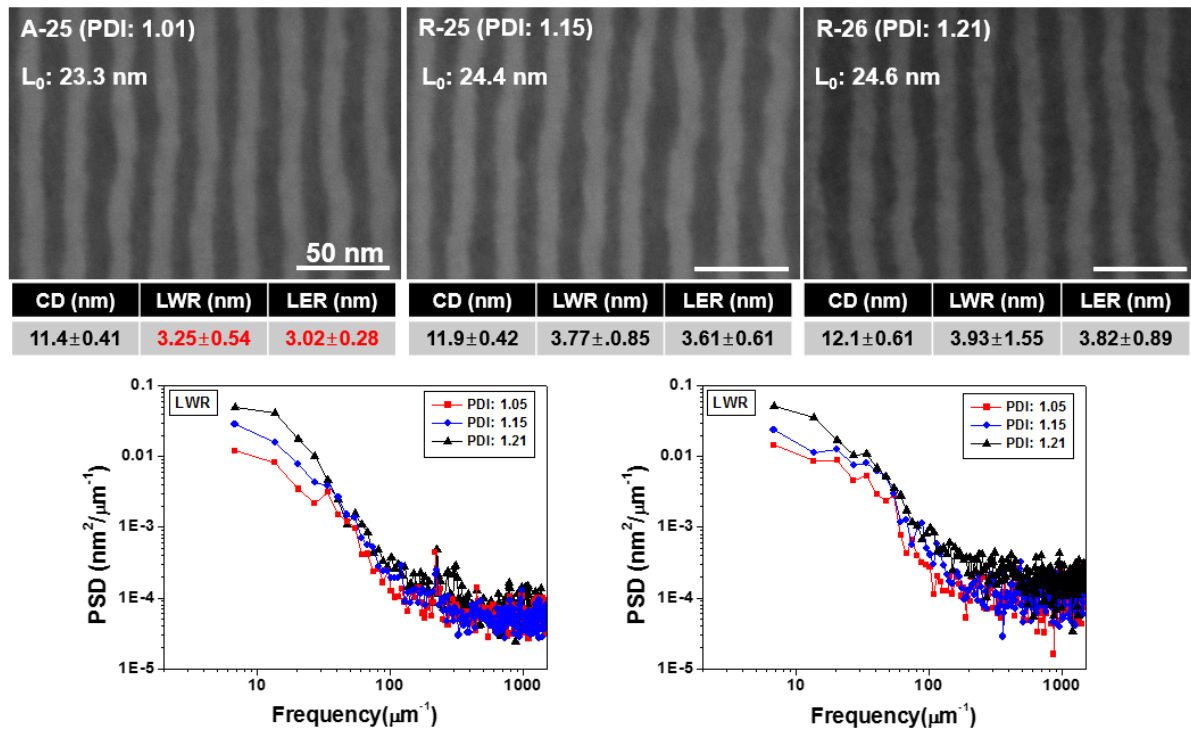


Figure S13. Pattern quality comparison of PS-*b*-P4BDSS by changing PDI

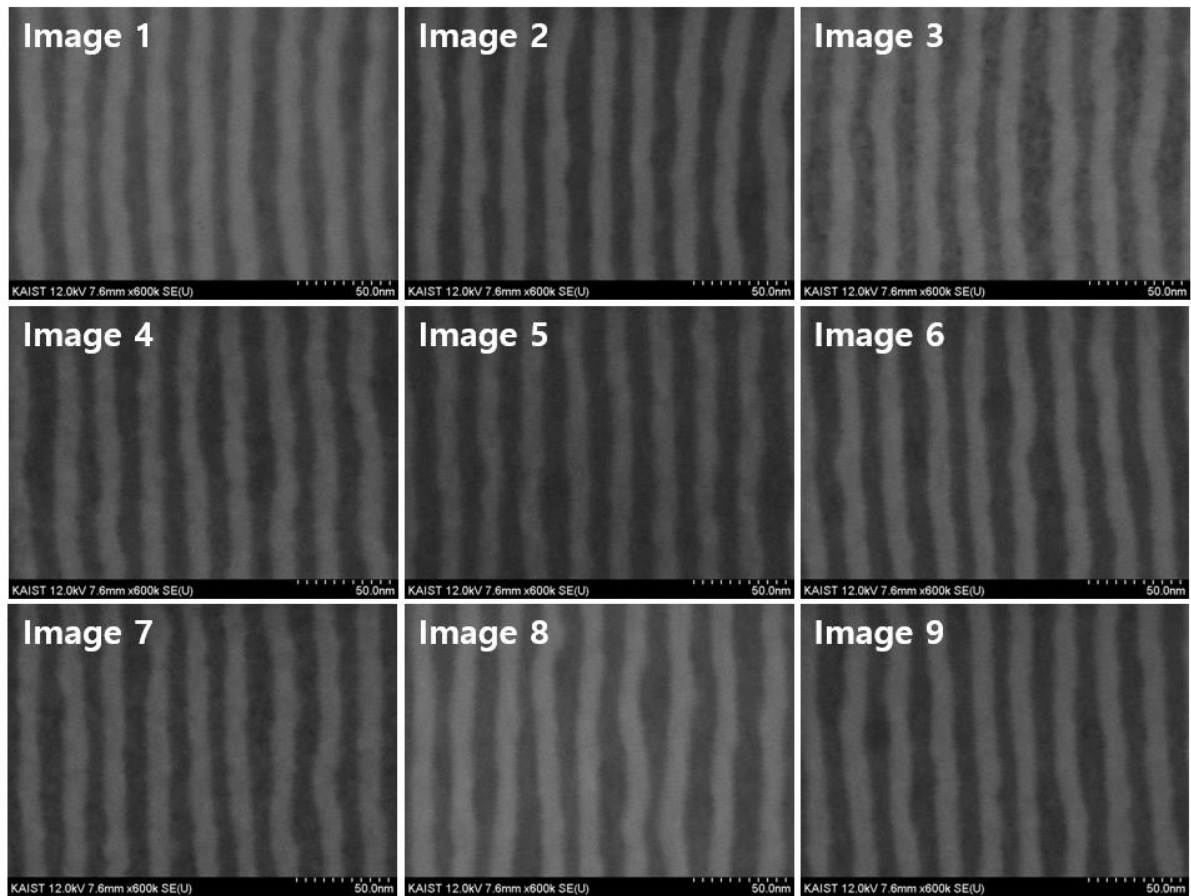


Figure S14. Pattern quality analysis of A-25

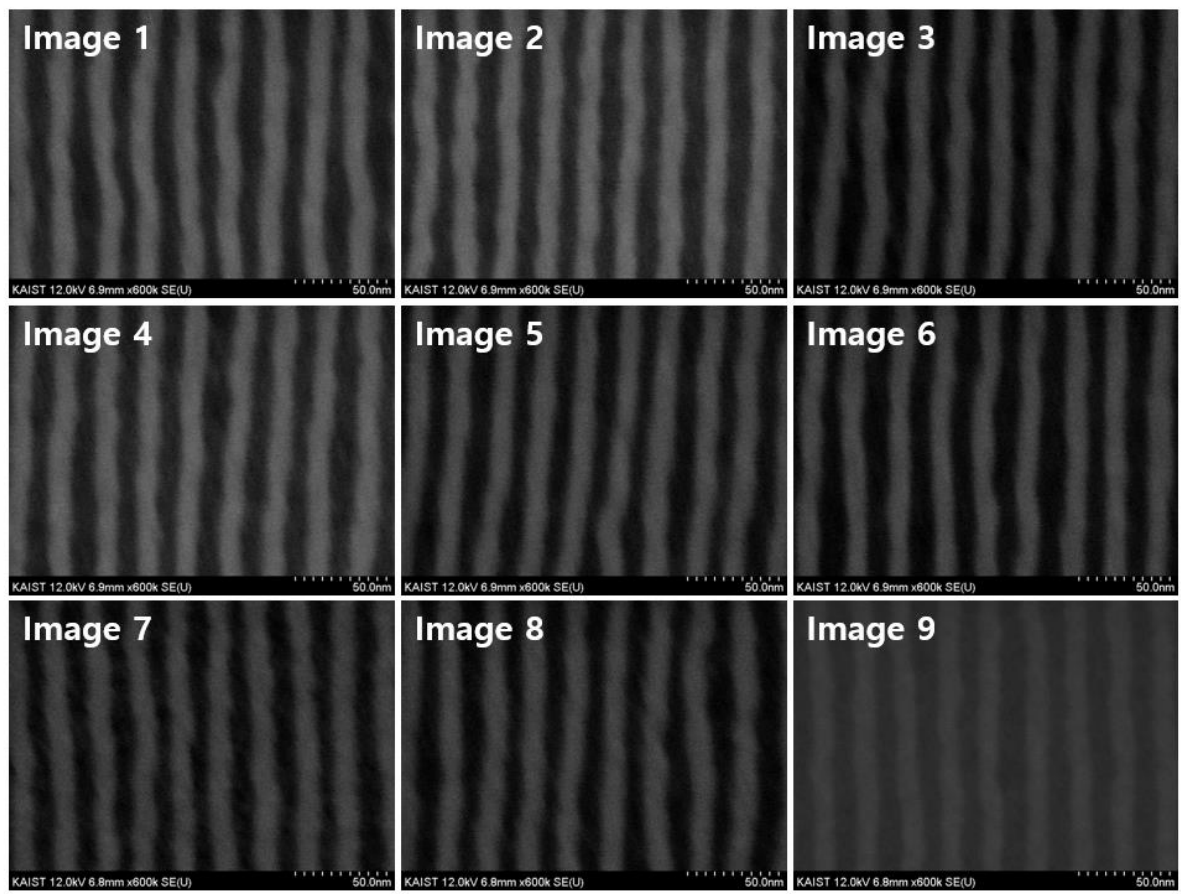


Figure S15. Pattern quality analysis of R-25

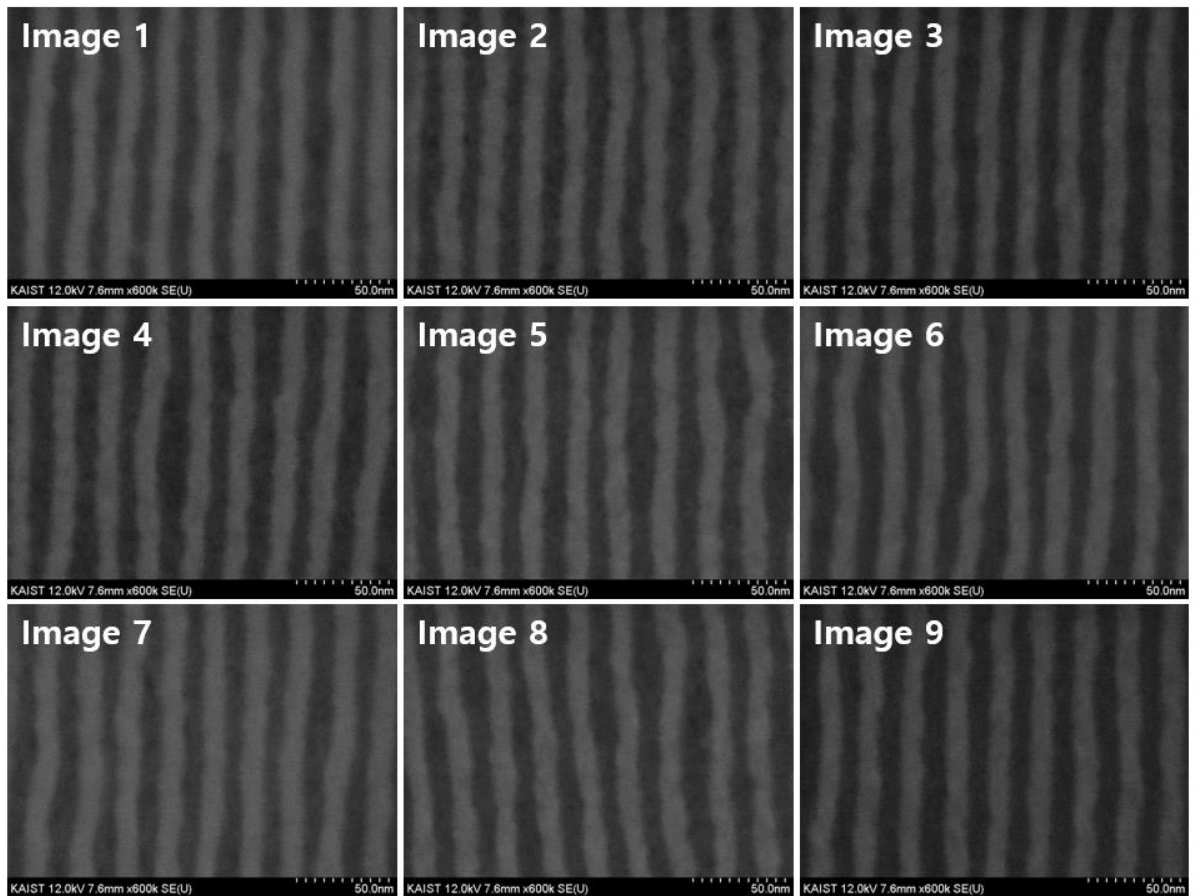


Figure S16. Pattern quality analysis of R-26

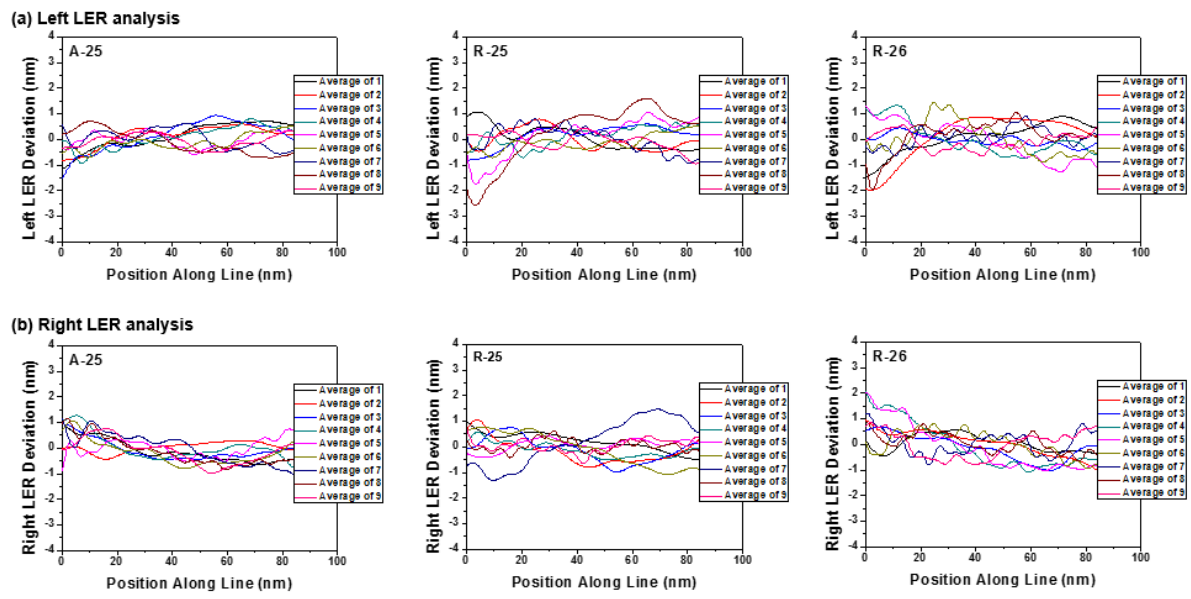


Figure S17. LER comparison of PS-*b*-P4BDSS

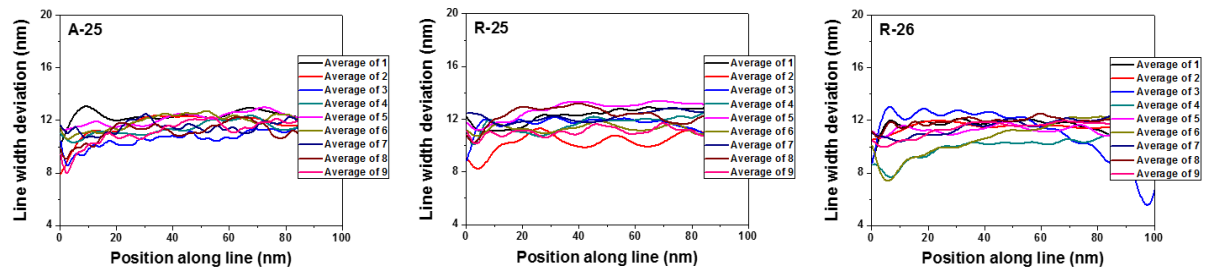


Figure S18. LWR comparison of PS-*b*-P4BDSS